01 Apr 2023

A New Approach to Proper Orthogonal Decomposition with Difference Quotients

Sarah Locke Eskew

John R. Singler
Missouri University of Science and Technology, singlerj@mst.edu

Recommended Citation

S. L. Eskew and J. R. Singler, "A New Approach to Proper Orthogonal Decomposition with Difference Quotients," *Advances in Computational Mathematics*, vol. 49, no. 2, article no. 13, Springer, Apr 2023. The definitive version is available at https://doi.org/10.1007/s10444-023-10011-9

Adv Comput Math (2023) 49:13
https://doi.org/10.1007/s10444-023-10011-9

A new approach to proper orthogonal decomposition with difference quotients

Sarah Locke Eskew[1] · **John R. Singler**[2]

Received: 19 October 2021 / Accepted: 9 January 2023

Abstract

In a recent work (Koc et al., SIAM J. Numer. Anal. **59**(4), 2163–2196, 2021), the authors showed that including difference quotients (DQs) is necessary in order to prove optimal pointwise in time error bounds for proper orthogonal decomposition (POD) reduced order models of the heat equation. In this work, we introduce a new approach to including DQs in the POD procedure. Instead of computing the POD modes using all of the snapshot data and DQs, we only use the first snapshot along with all of the DQs and special POD weights. We show that this approach retains all of the numerical analysis benefits of the standard POD DQ approach, while using a POD data set that has approximately half the number of snapshots as the standard POD DQ approach, i.e., the new approach requires less computational effort. We illustrate our theoretical results with numerical experiments.

Keywords Proper orthogonal decomposition · Projections · Approximation theory · Difference quotients · Reduced order models

Mathematics Subject Classification (2010) 35A01 · 65L10 · 65L12 · 65L20 · 65L70

Communicated by: Stefan Volkwein

John R. Singler contributed equally to this work.

✉ Sarah Locke Eskew
sarklock@utsouthern.edu

John R. Singler
singlerj@mst.edu

[1] School of Mathematics and Science, University of Tennessee Southern, 433 W Madison Street, Pulaski, TN, 38478, USA

[2] Department of Mathematics and Statistics, Missouri University of Science and Technology, 400 W. 12th Street, Rolla, MO, 65401, USA

Published online: 20 February 2023

1 Introduction

A common model order reduction technique used for approximating partial differential equations (PDEs) and other mathematical models is proper orthogonal decomposition (POD). With this method, data from simulations or experiments are used to create modes, which are then used in a projection method to create a reduced order model (ROM). Because of the efficiency of POD ROMs, they are used in many applications including control theory and fluid dynamics to solve computationally demanding problems. For a small selection of applications, see, e.g., [1, 3, 11, 15, 21, 24, 25, 28, 33, 39, 43, 44, 49].

Because of the widespread use of POD in applications, many researchers have studied POD ROMs from a numerical analysis perspective (see, e.g., [5, 22, 23, 31, 32, 37, 38, 41, 47]). In order for POD to be beneficial for applications, researchers must understand how the various errors involved behave. To fully understand this for PDEs, three types of error must be considered: spatial discretization error, time discretization error, and ROM discretization error. The optimality of these errors is of particular concern. POD numerical analysis papers tend to focus on the time discretization error and the ROM discretization error since the analysis of these errors contain POD-specific features. In contrast, the spatial discretization error can typically be handled using existing techniques. For more information on these three types of error and the numerical analysis of POD, including a history and a discussion of POD-specific features in the error analysis, see the introduction of the recent work [29]. The current work focuses only on the POD ROM errors and leads to an improved understanding of the numerical analysis of POD ROMs, particularly in regards to difference quotients and pointwise error bounds.

There are multiple approaches to creating POD modes from the data. In this work, two of the most common existing methods are considered, and we introduce a new method. The first existing approach is a standard method to compute the POD modes and uses only the data, and the second existing approach utilizes both the data and the difference quotients (DQs) of the data. Researchers originally started including DQs in the POD calculations to improve the numerical analysis results for POD reduced order models as in [31]. Furthermore, DQs have been used in many applications including [14, 16, 20, 24, 27, 30, 35, 45, 50]. For years, researchers have been curious about the role DQs play in the behavior of the ROM and whether or not they should be included in the POD computations. In general, results on this topic were inconclusive. However in 2014, substantial progress was made by Iliescu and Wang in [22] towards answering this question. In this work a notion of optimality was introduced and results strongly suggested that DQs were needed to achieve optimal pointwise-in-time convergence rates. Recently in [29], further progress was made. In this work, it is shown that a critical assumption concerning pointwise POD projection errors often made when using standard POD without DQs is automatically guaranteed to be satisfied when DQs are included with the data (see Theorem 3 below). The notion of optimality introduced in [22] is extended, and it is shown that including difference quotients results in pointwise POD projection error bounds and optimal pointwise ROM errors. The goal of the current work is to further investigate and understand pointwise error bounds in the POD-ROM setting.

To do this, we introduce a new approach to deriving POD modes from the data. When using all of the data with all of the DQs, the resulting data set is linearly dependent, i.e., the data set being used contains redundant information. This also leads to more costly POD basis computations compared to standard POD without DQs. In order to improve this situation, we consider the following question: Can we obtain all of the same numerical analysis benefits of using DQs with POD using a data set without redundancy? We show that the answer is yes, if we choose the data set and POD weights in a correct way. For our new approach, we use only the first data snapshot and all of the difference quotients. This new approach to using DQs with POD uses a data set without redundancy in the following sense: if the original set of M snapshots is linearly independent, then the data set used in our new DQ approach has dimension M and is also linearly independent. Using this new collection of data and special POD weights, we are not only able to approximate the DQs and the one regular snapshot, but all of the other regular snapshot data as well. With this method, we also prove that we retain the numerical analysis benefits that come with having the DQs in the POD data set.

The rest of the work is organized as follows. First, we introduce the details for both current approaches to POD in Section 2. Then, we describe our new computational approach in Section 3 and also prove POD data approximation error formulas, present preliminary computations, and prove pointwise POD data approximation error results. This is followed by reduced order model error analysis in Section 4 and results from more detailed numerical computations in Section 5.

2 Proper orthogonal decomposition

In this section, we introduce current approaches to POD: the standard POD approach and standard POD with difference quotients approach. We compare our new method to known results about these established methods throughout the work. For details on the basics of POD, see, e.g., [6, 13, 19, 32, 36, 40, 48].

First, we establish some general notation. Let M and N be positive integers and let X and Y be separable Hilbert spaces where the space X is called the POD space. It is possible for $Y = X$. We do not assume any relationship between the spaces; e.g., we do not assume Y is a subset of X or any other condition. However, we frequently consider cases where a given data set is contained in both X and Y.

In the examples in this work for these Hilbert spaces we use the standard function spaces $L^2(\Omega)$ and $H_0^1(\Omega)$, where Ω is the spatial domain. Note that we allow for any combination of X and Y in regards to the standard function spaces, i.e., $X = L^2(\Omega)$ or $X = H_0^1(\Omega)$ and $Y = L^2(\Omega)$ or $Y = H_0^1(\Omega)$.

Furthermore, let $\mathbb{K} = \mathbb{R}$ or $\mathbb{K} = \mathbb{C}$. In order to consider variable weights that often arise with numerical integration, we define $S := \mathbb{K}_\Gamma^M$ with the weighted inner product given by

$$(g, h)_S = h^* \Gamma g = \sum_{j=1}^{M} \gamma_j g^j \overline{h^j}$$

where $g, h \in S$, $\Gamma = \text{diag}(\gamma_1, \gamma_2, \ldots, \gamma_M)$, and the values $\{\gamma_j\}_{j=1}^M$ are positive weights. In some instances, it is beneficial to take the positive weights to be certain specific values in order to approximate various time integrals.

For the POD reduced order modeling in this work, we consider data sets consisting of approximate solution data for a time dependent partial differential equation. Throughout, we consider the time interval $[0, T]$ with $T > 0$ a fixed positive constant. The approximate solution data will be given at times $t_n = (n-1)\Delta t$, for $n = 1, \ldots, N$, where the time step is given by $\Delta t = \frac{T}{N-1}$. Note that while T is fixed, N can vary.

This work also uses projections. For a normed space Z, a bounded linear operator $\Pi : Z \to Z$ is a *projection* onto $Z_r \subset Z$ if $\Pi^2 = \Pi$ and the range of Π is Z_r. Then, $\Pi z = z$ for any $z \in Z_r$. Note that we do not assume that a projection is orthogonal unless explicitly stated.

Further details and a selection of known results for the standard POD approach and the standard approach to POD including difference quotients can be found in Sections 2.1 and 2.2 respectively.

2.1 Standard POD

First, we introduce the standard POD problem and operator. For this POD problem, difference quotients are not considered. Let $W = \{w^j\}_{j=1}^M \subset X$ be the POD data, also called the POD snapshots, for some integer $M > 0$. Given $r > 0$, the standard POD problem is to find an orthonormal basis $\{\varphi_j\}_{j=1}^r \subset X$, also called the POD basis, minimizing the data approximation error

$$E_r = \sum_{j=1}^{M} \gamma_j \|w^j - \Pi_r^X w^j\|_X^2. \tag{1}$$

Here, the operator $\Pi_r^X : X \to X$ is the orthogonal projection onto the subset X_r of the POD space X given by $X_r = \text{span}\{\varphi_k\}_{k=1}^r$ defined by

$$\Pi_r^X x = \sum_{k=1}^{r} (x, \varphi_k)_X \varphi_k. \tag{2}$$

The operator that provides the solution to this problem is $K : S \to X$ which is given by

$$Kf = \sum_{j=1}^{M} \gamma_j f^j w^j, \quad f = [f^1, f^2, \ldots, f^M]^T. \tag{3}$$

We call this operator the standard POD operator. This operator K is compact and has a singular value decomposition given by $\{\lambda_k^{1/2}, f_k, \varphi_k\} \subset \mathbb{R} \times S \times X$ where $\{\lambda_k^{1/2}\}$ are the singular values and $\{f_k\}$ and $\{\varphi_k\}$ are the (nonunique) orthonormal singular vectors. Here, we use the notation f_k to denote the kth singular vector in S, and the jth entry of this vector is denoted by f_k^j. We can write $Kf_k = \lambda_k^{1/2}\varphi_k$. The singular vectors $\{\varphi_k\}$ are called the POD modes of the data $\{w^k\} \subset X$ and $\{\lambda_k^{1/2}\}$ are called the POD singular values. For more information about the singular value

decomposition of compact operators, see, e.g., [10, Chapters VI–VIII], [26, Section V.2.3], [34, Chapter 30], [42, Sections VI.5–VI.6].

The POD modes provide the best low rank approximation to the data, and it is known that

$$E_r = \sum_{j=1}^{M} \gamma_j \|w^j - \Pi_r^X w^j\|_X^2 = \sum_{k=r+1}^{s} \lambda_k \tag{4}$$

where $\{\lambda_k\}$ are the POD eigenvalues and s is the number of positive POD singular values.

For certain choices of weights $\{\gamma_i\}$ the error given in Equation (1) approximates a time integral, or a constant multiple of a time integral, as more and more time steps are used. Using various quadrature rules to determine the appropriate POD weights will lead to different time integral approximations. For various choices of weights or quadrature rules (leading to a convergent approximation to a time integral in an appropriate sense), convergence results for POD eigenvalues, POD modes, and the best low rank error Equation (4) can be found in [9, 13, 32, 46].

At this point, we do not specify any particular choice for the (positive) weights. This allows us to apply a known result (Lemma 1 below) to obtain results for different POD approaches with specific (possibly nonstandard) fixed weights, as we see with the new POD with difference quotients method introduced in Section 3.

The following lemma provides exact formulas for POD data approximation errors using other norms and other projections. As mentioned above, we use this result later to provide POD data approximation results for other POD approaches. The proof of Lemma 1 is similar to existing proofs of closely related results that exist in the literature so we omit the proof here (see, e.g., [29, Lemma 2.2], [37, Theorem 5.1]).

Lemma 1 *Let X and Y be separable Hilbert spaces, $W = \{w^j\}_{j=1}^M \subset X$, $X_r = \operatorname{span}\{\varphi_k\}_{k=1}^r$, and $\Pi_r^X : X \to X$ be the orthogonal projection onto X_r. Let s be the number of positive POD singular values for K defined in* Equation (3)*. If $W \subset Y$, then*

$$\sum_{j=1}^{M} \gamma_j \|w^j - \Pi_r^X w^j\|_Y^2 = \sum_{i=r+1}^{s} \lambda_i \|\varphi_i\|_Y^2. \tag{5}$$

In addition, if $\pi_r : Y \to Y$ is any bounded linear projection onto X_r, then

$$\sum_{j=1}^{M} \gamma_j \|w^j - \pi_r w^j\|_Y^2 = \sum_{i=r+1}^{s} \lambda_i \|\varphi_i - \pi_r \varphi_i\|_Y^2. \tag{6}$$

The formula given in Equation (6) is the most general case. Recall that it is possible for $X = Y$. Therefore, Equation (6) holds with $Y = X$ if $\pi_r : X \to X$ is some bounded linear projection that is not necessarily the orthogonal projection onto X_r. In the computations, we specify the spaces X and Y as well as the projection π_r.

The standard POD approach does not have general bounds for pointwise errors, as shown in [29, Section 3].

2.2 POD with difference quotients

Another common approach to POD involves the use of difference quotients. Throughout this work, we refer to this method as the standard DQ approach. This approach has been studied by many including [12, 18, 22, 29–31]. In this work we consider backward Euler for the time stepping scheme and the difference quotients.

Let $U = \{u^j\}_{j=1}^N \subset X$ be a given data set. Then, the problem is to find an orthonormal basis minimizing the error

$$E_r^{DQ} = \sum_{j=1}^{N} \Delta t \|u^j - \Pi_r^X u^j\|_X^2 + \sum_{j=1}^{N-1} \Delta t \|\partial u^j - \Pi_r^X \partial u^j\|_X^2 \tag{7}$$

where Δt is the time step and the difference quotients are given by

$$\partial u^j = \frac{u^{j+1} - u^j}{\Delta t}. \tag{8}$$

These difference quotients approximate the time derivative of the data in continuous time. Note that if u is a continuously differentiable function in time that takes value in X and if $u^j = u(t_j)$ for all j, where $t_j = (j-1)\Delta t$, then the error in Equation (7) can be thought of as a left Riemann sum approximation to the following time integral:

$$\int_0^{T_1} \|u(t) - \Pi_r^X u(t)\|_X^2 \, dt + \int_0^T \|\partial_t u(t) - \Pi_r^X \partial_t u(t)\|_X^2 \, dt,$$

where $T_1 = T + \Delta t$, $T = (N-1)\Delta t$, ∂_t denotes the derivative with respect to time, and we assume ∂u^j approximates $\partial_t u(t_j)$.

The operator that provides the minimizing basis for the error in Equation (7) is $K_{DQ} : S \to X$ defined by

$$K_{DQ} f = \sum_{j=1}^{N} \Delta t f^j u^j + \sum_{j=1}^{N-1} \Delta t f^{N+j} \partial u^j. \tag{9}$$

This approach uses a total of $M = 2N - 1$ data snapshots which is nearly twice as many as the standard POD approach. Note for this operator we have $K_{DQ} f = Kf$ where $w^i = u^i$ and $\gamma_i = \Delta t$ for $i = 1, \ldots N$, and also $w^{N+i} = \partial u^i$ and $\gamma_{N+i} = \Delta t$ for $i = 1, \ldots, N-1$. The resulting POD data set is $\{w^j\}_{j=1}^M$, where $M = 2N - 1$. Taking $\{\lambda_j^{DQ}\}_{j=1}^{2N-1}$ to be the POD eigenvalues and keeping the same notation $\{\varphi_j\}$ for the POD basis functions, we get similar results to those for the standard POD operator. When using this new set $\{w^j\}$ as the POD data set, we not only have a set that is nearly twice as large as the original but it can also be checked that the new set is linearly dependent. This redundancy is something we avoid with our new approach introduced in Section 3.

Remark 1 While the weights can be taken to be any set of positive constants, for simplicity in this work we take them to be the constant Δt. The results in this work can be extended to variable weights or other choices of constant weights. One popular choice of constant weight in the literature is M^{-1} as in [22, 29] where M represents

the total number of data snapshots for the standard difference quotient approach to POD. Similar to the standard POD case, with certain choices of weights, one can approximate time integrals with various quadrature rules.

The following result is also similar to Lemma 2.4 in [29]. We provide it here for completeness.

Lemma 2 *Let X and Y be separable Hilbert spaces and $U = \{u^j\}_{j=1}^N \subset X$, $X_r = \text{span}\{\varphi_k\}_{k=1}^r$ and $\Pi_r^X : X \to X$ be the orthogonal projection onto X_r. Let s be the number of positive POD singular values for K_{DQ} defined in* Equation (9)*. We have the following error formula:*

$$\sum_{j=1}^{N} \Delta t \|u^j - \Pi_r^X u^j\|_X^2 + \sum_{j=1}^{N-1} \Delta t \|\partial u^j - \Pi_r^X \partial u^j\|_X^2 = \sum_{i=r+1}^{s} \lambda_i^{DQ}. \tag{10}$$

If $U = \{u^j\}_{j=1}^N \subset Y$, then

$$\sum_{j=1}^{N} \Delta t \|u^j - \Pi_r^X u^j\|_Y^2 + \sum_{j=1}^{N-1} \Delta t \|\partial u^j - \Pi_r^X \partial u^j\|_Y^2 = \sum_{i=r+1}^{s} \lambda_i^{DQ} \|\varphi_i\|_Y^2. \tag{11}$$

In addition, if $\pi_r : Y \to Y$ is any bounded linear projection onto X_r, then

$$\sum_{j=1}^{N} \Delta t \|u^j - \pi_r u^j\|_Y^2 + \sum_{j=1}^{N-1} \Delta t \|\partial u^j - \pi_r \partial u^j\|_Y^2 = \sum_{i=r+1}^{s} \lambda_i^{DQ} \|\varphi_i - \pi_r \varphi_i\|_Y^2. \tag{12}$$

Proof This result follows from Equation (4) and Lemma 1 by taking $\{\lambda_j^{DQ}\}_{j=1}^s$ as the POD eigenvalues for the POD operator in Equation (9). □

We have the following result about the pointwise error bounds for this POD case. A similar result with a different set of constant weights can be found in [29, Theorem 3.7]. The proof of the result below is similar so we omit it here. That theorem was key to obtaining the optimal pointwise POD ROM error bounds which were a main contribution of that work.

Theorem 3 *Let X and Y be separable Hilbert spaces and $U = \{u^j\}_{j=1}^N \subset X$, $X_r = \text{span}\{\varphi_k\}_{k=1}^r$ and $\Pi_r^X : X \to X$ be the orthogonal projection onto X_r. Let s be the number of positive POD singular values for K_{DQ}. We have*

$$\max_{1 \le j \le N} \|u^j - \Pi_r^X u^j\|_X^2 \le C \left(\sum_{i=r+1}^{s} \lambda_i^{DQ} \right). \tag{13}$$

If $U = \{u^j\}_{j=1}^N \subset Y$, *then*

$$\max_{1\le j\le N} \|u^j - \Pi_r^X u^j\|_Y^2 \le C\left(\sum_{i=r+1}^{s} \lambda_i^{DQ} \|\varphi_i\|_Y^2\right). \tag{14}$$

If $\pi_r : Y \to Y$ *is any bounded linear projection onto* X_r, *then*

$$\max_{1\le j\le N} \|u^j - \pi_r u^j\|_Y^2 \le C\left(\sum_{i=r+1}^{s} \lambda_i^{DQ} \|\varphi_i - \pi_r \varphi_i\|_Y^2\right) \tag{15}$$

where $C = 2\max\{T^{-1}, T\}$.

In Section 3.2, we obtain a similar pointwise POD projection error result for the new POD approach described below in Section 3.

3 A new approach to POD with difference quotients

Next, we return to the question posed in the introduction: "Can we obtain all of the same numerical analysis benefits of using DQs with POD using a data set without redundancy?" We obtain a positive answer to this question by introducing a new POD problem and operator. Instead of including all of the POD data snapshots and all of the difference quotients as in Section 2.2, we include the first data snapshot and all of the difference quotients. Thus for the data $U = \{u^j\}_{j=1}^N \subset X$, the new POD problem is to minimize the error given by

$$E_r^{DQ1} = \|u^1 - \Pi_r^X u^1\|_X^2 + \sum_{j=1}^{N-1} \Delta t \|\partial u^j - \Pi_r^X \partial u^j\|_X^2 \tag{16}$$

where the difference quotients are defined by Equation (8). Note that the POD error function in Equation (16) does not include the weighted sum of the errors of the regular snapshots; this contrasts with the POD approaches in Section 2, which both include such error terms (see Equations (1) and Equation (7)). Furthermore, in the POD approaches in Section 2, we have exact error formulas for these error terms (see Lemma 1 and 2). In Section 3.2, we consider the weighted sum of the errors of the regular snapshots for this new approach and obtain an approximation error result in Corollary 8.

Similar to the standard POD DQ approach in Section 2.2, if $u^j = u(t_j)$ then the error in Equation (16) can be thought of as a left Riemann sum approximation to the following error measure involving a time integral:

$$\|u(0) - \Pi_r^X u(0)\|_X^2 + \int_0^T \|\partial_t u(t) - \Pi_r^X \partial_t u(t)\|_X^2 \, dt,$$

where $T = (N-1)\Delta t$, ∂_t denotes the derivative with respect to time, and we assume ∂u^j approximates $\partial_t u(t_j)$.

Note that with this approach, we have a total of $N-1$ difference quotients. Together with the single snapshot, we have a total of N data snapshots for this POD problem. This is an improvement with regard to reducing the number of data snapshots from the standard DQ approach to POD, which has $2N-1$ data snapshots.

The minimum error can be found using the POD operator:

$$K_1 f = f^1 u^1 + \sum_{j=1}^{N-1} \Delta t f^{j+1} \partial u^j \tag{17}$$

We have $K_1 f = Kf$ where $w^1 = u^1$, $\gamma_1 = 1$, $\gamma_{i+1} = \Delta t$, and $w^{i+1} = \partial u^i$ for $i = 1, \ldots, N-1$. We choose to use the constant time step, Δt, as the weight for simplicity throughout the work. The results can be extended to include variable weights as well. Recall that for certain choices of weights one can approximate a time integral and the difference quotients approximate a time derivative.

Note that in contrast to the data set created for the standard POD approach with DQs, the data set for this new approach is linearly independent if the original data set is linearly independent as shown in Lemma 4.

Lemma 4 *If $\{u^i\}_{i=1}^N$ is linearly independent then $\{w^i\}_{i=1}^N$ given by $w^1 = u^1$ and $w^{i+1} = \partial u^i$ for $i = 1, \ldots, N-1$ is linearly independent.*

Proof We show that if

$$c_1 w^1 + c_2 w^2 + \cdots + c_N w^N = 0$$

then $c_i = 0$ for all $i = 1, \ldots, N$. We have

$$c_1 u^1 + c_2 \left(\frac{u^2 - u^1}{\Delta t} \right) + \cdots + c_i \left(\frac{u^i - u^{i-1}}{\Delta t} \right) + \cdots + c_N \left(\frac{u^N - u^{N-1}}{\Delta t} \right) = 0$$

then

$$\left(c_1 - \frac{c_2}{\Delta t} \right) u^1 + \left(\frac{c_2}{\Delta t} - \frac{c_3}{\Delta t} \right) u^2 + \cdots + \left(\frac{c_{N-1}}{\Delta t} - \frac{c_N}{\Delta t} \right) u^{N-1} + \frac{c_N}{\Delta t} u^N = 0.$$

Since $\{u^i\}$ is linearly independent we know each of these coefficients must equal 0. Solving that system of equations leads to the conclusion that $c_i = 0$ for all $i = 1, \ldots, N$. □

If we let $\{\lambda_j^{DQ1}\}_{j=1}^N$ be the POD eigenvalues for this new POD approach, and let $\{\varphi_k\}_{k=1}^r$ be the POD modes for this data, we get the following error formulas given in Lemma 5.

Lemma 5 *Let X and Y be separable Hilbert spaces and $U = \{u^j\}_{j=1}^N \subset X$, $X_r = \text{span}\{\varphi_k\}_{k=1}^r$ and $\Pi_r^X : X \to X$ be the orthogonal projection onto X_r. Let s be the*

number of positive POD singular values for K_1 defined in Equation (17). *We have the following formula for the data approximation error:*

$$\|u^1 - \Pi_r^X u^1\|_X^2 + \sum_{j=1}^{N-1} \Delta t \|\partial u^j - \Pi_r^X \partial u^j\|_X^2 = \sum_{i=r+1}^{s} \lambda_i^{DQ1}. \tag{18}$$

If $U = \{u^j\}_{j=1}^N \subset Y$, then

$$\|u^1 - \Pi_r^X u^1\|_Y^2 + \sum_{j=1}^{N-1} \Delta t \|\partial u^j - \Pi_r^X \partial u^j\|_Y^2 = \sum_{i=r+1}^{s} \lambda_i^{DQ1} \|\varphi_i\|_Y^2. \tag{19}$$

If in addition $\pi_r : Y \to Y$ is any bounded linear projection onto X_r, then

$$\|u^1 - \pi_r u^1\|_Y^2 + \sum_{j=1}^{N-1} \Delta t \|\partial u^j - \pi_r \partial u^j\|_Y^2 = \sum_{i=r+1}^{s} \lambda_i^{DQ1} \|\varphi_i - \pi_r \varphi_i\|_Y^2. \tag{20}$$

Proof This result follows from Equation (4) and Lemma 1 by taking $\{\lambda_j^{DQ1}\}_{j=1}^s$ as the POD eigenvalues for the POD operator in Equation (17). □

Preliminary computational results and pointwise error estimates for this new POD approach are discussed in Sections 3.1 and 3.2 respectively.

3.1 Preliminary computations

Before moving to our main results we perform some preliminary computations to test the new POD approach with difference quotients. For all computations throughout this work, we consider the following test problem.

Test Problem: Consider the one dimensional heat equation

$$\begin{aligned} u_t - \nu u_{xx} &= 0, \text{ in } \Omega \times [0, T] \\ u(x, 0) &= e^x \sin(\pi x) \end{aligned}$$

with $\nu = 1$, $\Omega = [0, 1]$, $T = 1$, and zero Dirichlet boundary conditions.

For the data $\{u^j\}$, we compute the solution using the finite element method with linear elements, equally spaced nodes, and backward Euler with a constant time step for the time marching scheme. The initial condition is taken to be the linear interpolation of the initial condition with respect to the finite element nodes. For the POD space $X = L^2(\Omega)$, since the data is finite dimensional we can calculate the POD modes, POD singular values, and the data approximation errors exactly which allows for comparison between the errors in the formulas from Lemma 5 and the actual approximation errors. In order to compute the singular value decomposition (SVD) of the POD operator, we use the technique described in [8, Section 2.2] with a minor modification to account for the POD weights. This procedure works well and is highly accurate for smaller data sets; for larger data sets, one could use an incremental SVD approach or another related algorithm instead (see, e.g., [2, 4, 7, 8, 17] and the references therein).

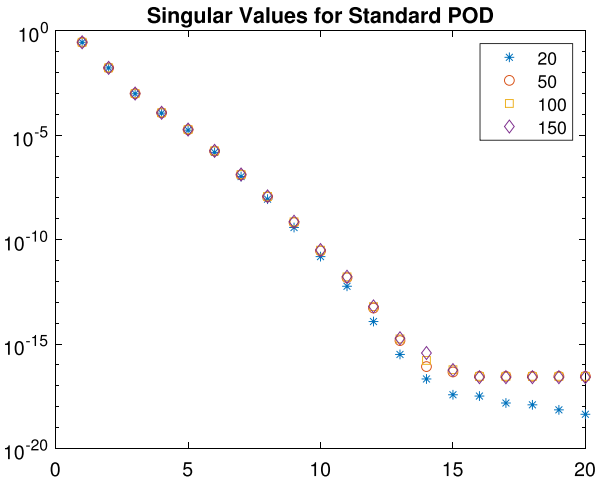

Fig. 1 Plot of singular values of the standard POD operator using different numbers of finite element nodes

First, we plot the singular values for both the standard POD and our new POD approach that includes one data snapshot and all of the difference quotients. For the standard POD computations, we use the data set consisting of only the regular snapshots $w^j = u^j$ for $j = 1, ..., N$ and we choose constant weights $\gamma_j = \Delta t$ for $j = 1, \ldots, N$. The singular value plots allow for a quick comparison between the two approaches to POD and are given in Figs. 1 and 2. For each plot, we show the first 20 POD singular values for 20, 50, 100, and 150 finite element nodes when using 100 equally spaced time steps. From these plots, we see the POD singular values decay

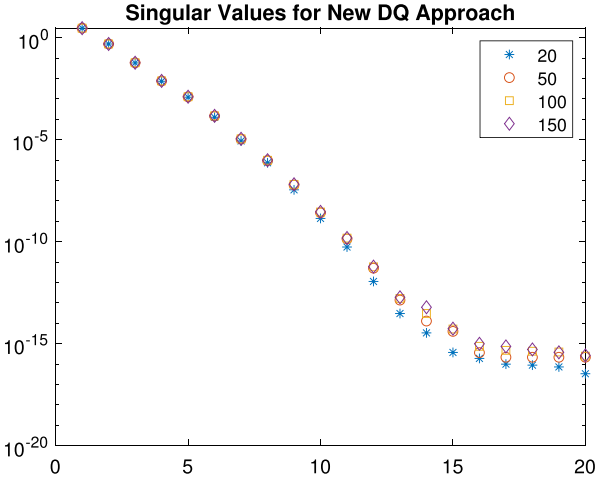

Fig. 2 Plot of singular values of the new difference quotient POD operator using different numbers of finite element nodes

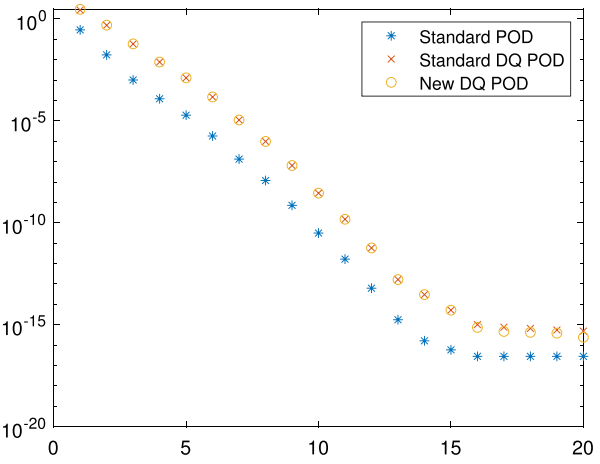

Fig. 3 Plot of singular values of the new difference quotient POD operator, the standard POD operator, and the standard difference quotient POD operator

at a similar rate which indicates that the POD basis for each case has a similar ability to approximate the data.

Furthermore, Fig. 3 shows the singular values for all three approaches with 100 equally spaced time steps and 100 finite element nodes. We again see that the singular values decay at a similar rate, as noted above. The figure also shows that the singular values for the new DQ approach are larger in magnitude than the standard approach for this specific example, but are very similar in magnitude to the standard DQ approach.

Next, we consider the data approximation error results given in Lemma 5 numerically. For these computations, we take 200 equally spaced time steps and 100 equally spaced finite element nodes and compute the actual errors and the error formulas. Recall that $X = L^2(\Omega)$ is the POD space and note that here we take either $Y = H_0^1(\Omega)$ or $Y = L^2(\Omega)$ with $(g,h)_{H_0^1} = (\nabla g, \nabla h)_{L^2}$. When $Y = L^2(\Omega)$, we have $X = Y$ and Equation (18) and Equation (19) are the same. Also note the projection π_r is taken to be the Ritz projection, which we discuss in more detail in Section 4. The results are shown for all formulas of Lemma 5 in Table 1 for $r = 4$, $r = 6$, and $r = 8$ with references given to the appropriate equation from the lemma. For example, the second row for each r value in the table gives the values for

$$\text{actual error} = \|u^1 - \Pi_r^X u^1\|_{H_0^1}^2 + \sum_{j=1}^{N-1} \Delta t \|\partial u^j - \Pi_r^X \partial u^j\|_{H_0^1}^2,$$

and

$$\text{error formula} = \sum_{i=r+1}^{s} \lambda_i^{DQ1} \|\varphi_k\|_{H_0^1}^2$$

with the respective values for r. Round-off errors in the POD computations can cause very small imaginary parts to occur in the error formulas. Thus we report the absolute

Table 1 Actual error vs. error formulas from Lemma 5 for new DQ POD with $X = L^2(\Omega)$

r value	Equation	Projection	Error norm	Actual error	Error formula
4	Equation (18)	Π_r^X	$X = L^2(\Omega)$	9.761e–06	9.761e–06
	Equation (19)	Π_r^X	$Y = H_0^1(\Omega)$	6.200e–03	6.200e–03
	Equation (20)	π_r	$Y = L^2(\Omega)$	1.736e–05	1.736e–05
	Equation (20)	π_r	$Y = H_0^1(\Omega)$	3.100e–03	3.100e–03
6	Equation (18)	Π_r^X	$X = L^2(\Omega)$	5.482e–09	5.482e–09
	Equation (19)	Π_r^X	$Y = H_0^1(\Omega)$	1.036e–05	1.036e–05
	Equation (20)	π_r	$Y = L^2(\Omega)$	1.133e–08	1.133e–08
	Equation (20)	π_r	$Y = H_0^1(\Omega)$	5.159e–06	5.159e–06
8	Equation (18)	Π_r^X	$X = L^2(\Omega)$	1.557e–12	1.557e–12
	Equation (19)	Π_r^X	$X = H_0^1(\Omega)$	4.772e–09	4.772e–09
	Equation (20)	π_r	$X = L^2(\Omega)$	3.481e–12	3.481e–12
	Equation (20)	π_r	$X = H_0^1(\Omega)$	1.659e–09	1.659e–09

value of the computed error formulas. Note that the difference between the actual errors and the error formulas is unnoticeable to the given significant digits. These computational results verify what we show analytically. Similar results are achieved when using $X = H_0^1(\Omega)$.

Computational comparisons between all three of the methods can be found in Section 5.1 where we consider the errors in the reduced order models.

3.2 Pointwise error bounds

Using the technique from [29, Lemma 3.6], we establish the following lemma which allows us to directly prove the POD pointwise projection error bounds for the new DQ POD approach and an approximation error result for the weighted sum of the errors of the regular snapshots. These results are necessary to prove the reduced order model error bounds and show their optimality in Section 4.

Lemma 6 *Let $T > 0$, Z be a normed space, $\{z^j\}_{j=1}^N \subset Z$, and $\Delta t = T/(N-1)$. Then,*

$$\max_{1\le j\le N} \|z^j\|_Z^2 \le C\left(\|z^1\|_Z^2 + \sum_{\ell=1}^{N-1} \Delta t \|\partial z^\ell\|_Z^2\right) \tag{21}$$

where $\partial z^\ell = \frac{z^{\ell+1}-z^\ell}{\Delta t}$ for $\ell = 1, \ldots, N-1$, and $C = 2\max\{T, 1\}$.

Proof Note using $z^j = z^1 + \sum_{\ell=1}^{j-1} \Delta t\,(\partial z^\ell)$ and the Cauchy-Schwarz inequality we have

$$\|z^j\| \le \|z^1\| + \sum_{\ell=1}^{j-1} \Delta t \|\partial z^\ell\| \le \|z^1\| + \left(\sum_{\ell=1}^{j-1} \Delta t\right)^{1/2} \left(\sum_{\ell=1}^{N-1} \Delta t \|\partial z^\ell\|^2\right)^{1/2}.$$

Then, squaring both sides, using $(a+b)^2 \le 2a^2 + 2b^2$, and noting $\sum_{\ell=1}^{j-1} \Delta t \le \sum_{\ell=1}^{N-1} \Delta t = T$ gives

$$\|z^j\|^2 \le 2\|z^1\|^2 + 2\left(\sum_{\ell=1}^{j-1} \Delta t\right)\left(\sum_{\ell=1}^{N-1} \Delta t \|\partial z^\ell\|^2\right) \le 2\|z^1\|^2 + 2T \sum_{\ell=1}^{N-1} \Delta t \|\partial z^\ell\|^2.$$

Take the maximum over all j and the result follows. □

Next, we obtain a pointwise POD projection error result for the new POD DQ approach that is very similar to Theorem 3 for the standard POD DQ case.

Theorem 7 *Let X and Y be separable Hilbert spaces, $U = \{u^j\}_{j=1}^N \subset X$, $X_r = \text{span}\{\varphi_k\}_{k=1}^r$, and $\Pi_r^X : X \to X$ be the orthogonal projection onto X_r. Let s be the number of positive POD eigenvalues for U. Then,*

$$\max_{1\le j\le N} \|u^j - \Pi_r^X u^j\|_X^2 \le C\left(\sum_{i=r+1}^{s} \lambda_i^{DQ1}\right). \tag{22}$$

If $U = \{u^j\}_{j=1}^N \subset Y$, then

$$\max_{1\le j\le N} \|u^j - \Pi_r^X u^j\|_Y^2 \le C\left(\sum_{i=r+1}^{s} \lambda_i^{DQ1} \|\varphi_i\|_Y^2\right). \tag{23}$$

In addition, if $\pi_r : Y \to Y$ is any bounded linear projection onto X_r, then

$$\max_{1\le j\le N} \|u^j - \pi_r u^j\|_Y^2 \le C\left(\sum_{i=r+1}^{s} \lambda_i^{DQ1} \|\varphi_i - \pi_r \varphi_i\|_Y^2\right), \tag{24}$$

where $C = 2\max\{T, 1\}$.

Proof To prove this theorem take $z^j = u^j - \Pi_r^X u^j$ or $z^j = u^j - \pi_r u^j$ with $Z = X$ or $Z = Y$ in Lemma 6. For example, if we let $z^j = u^j - \Pi_r^X u^j$ and $Z = X$, then

$$\max_{1\le j\le N} \|u^j - \Pi_r^X u^j\|_X^2 \le C\left(\|u^1 - \Pi_r^X u^1\|_X^2 + \sum_{\ell=1}^{N-1} \Delta t \|\partial u^\ell - \Pi_r^X \partial u^\ell\|_X^2\right). \tag{25}$$

Applying Lemma 5 for each of the three cases gives the result. □

Next, we use the above pointwise error bounds to obtain error bounds for the weighted sum of the errors of the regular snapshots.

Corollary 8 *Let X and Y be separable Hilbert spaces, $U = \{u^j\}_{j=1}^N \subset X$, $X_r = \text{span}\{\varphi_k\}_{k=1}^r$, and $\Pi_r^X : X \to X$ be the orthogonal projection onto X_r. Let s be the number of positive POD eigenvalues for U. Then,*

$$\sum_{j=1}^{N} \Delta t \|u^j - \Pi_r^X u^j\|_X^2 \leq C \left(\sum_{i=r+1}^{s} \lambda_i^{DQ1} \right). \tag{26}$$

If $U = \{u^j\}_{j=1}^N \subset Y$, then

$$\sum_{j=1}^{N} \Delta t \|u^j - \Pi_r^X u^j\|_Y^2 \leq C \left(\sum_{i=r+1}^{s} \lambda_i^{DQ1} \|\varphi_i\|_Y^2 \right). \tag{27}$$

If in addition $\pi_r : Y \to Y$ is any bounded linear projection onto X_r, then

$$\sum_{j=1}^{N} \Delta t \|u^j - \pi_r u^j\|_Y^2 \leq C \left(\sum_{i=r+1}^{s} \lambda_i^{DQ1} \|\varphi_i - \pi_r \varphi_i\|_Y^2 \right), \tag{28}$$

where $C = 4 \max\{T^2, T\}$.

Proof Since

$$N\Delta t = \frac{N}{N-1}[(N-1)\Delta t] = [N/(N-1)]T \leq 2T,$$

we have

$$\sum_{j=1}^{N} \Delta t \|u^j - \Pi_r^X u^j\|_X^2 \leq 2T \max_{1 \leq j \leq N} \|u^j - \Pi_r^X u^j\|_X^2.$$

Theorem 7 gives Equation (26). The proofs of Equations (27) and (28) follow in the same way. □

These results are similar to those for the standard DQ approach while keeping redundancy out of the data set.

We note that considering different POD projections and different error norms allow us in the next section to obtain pointwise in time error estimates for POD model order reduction of the heat equation in different spatial norms and for different choices of the POD space X, namely, $X = L^2(\Omega)$ and $X = H_0^1(\Omega)$. In the literature, researchers have considered many different choices for X and many different choices for error norms to measure model order reduction quality for different PDEs. We adopted a general framework here so that our results may be applied in many different situations.

4 Reduced order modeling

In this section, we establish theory to compare the reduced order model solution to the backward Euler finite element solution for the heat equation using our new POD

with DQs approach. In this section, all POD computations are done using the new approach as presented in Section 3, and all function spaces are assumed to be real. Our analysis and proof techniques strongly rely on the approach in [29, Section 4]. We provide proofs to make the work self-contained.

Let $\Omega \subset \mathbb{R}^d$ with $d \geq 1$ be an open bounded domain with Lipschitz continuous boundary, and define $V = H_0^1(\Omega)$. The space V is a Hilbert space with inner product $(g, h)_{H_0^1} = (\nabla g, \nabla h)_{L^2}$. We consider the weak formulation of the heat equation with homogeneous Dirichlet boundary conditions:

$$(\partial_t u, v)_{L^2} + \nu(\nabla u, \nabla v)_{L^2} = (f, v)_{L^2} \quad \forall v \in V \tag{29}$$

where $u(\cdot, 0) = u^1$ is the initial condition, ν is a positive constant, and f is a given forcing function. We project Equation (29) onto a standard conforming finite element space $V^h \subset V$ and apply backward Euler to obtain the following discrete problem: given u^1, find $\{u^n\}_{n=2}^N$ such that

$$\left(\frac{u^{n+1} - u^n}{\Delta t}, v\right)_{L^2} + \nu(\nabla u^{n+1}, \nabla v)_{L^2} = (f^{n+1}, v)_{L^2} \quad \forall v \in V^h. \tag{30}$$

Here, for simplicity we assume the forcing f is continuous in time and f evaluated at any time is in $L^2(\Omega)$. Also, as is standard we define f^n to be the function f evaluated at time $t = t_n$.

We use the data set $\{u^n\}_{n=1}^N \subset V^h$ to compute the POD modes $\{\varphi_j\}_{j=1}^r \subset V^h$ using the new DQ approach with respect to the Hilbert space X. Below we take X to be either $X = L^2(\Omega)$ or $X = H_0^1(\Omega)$. Let $V_r^h = \text{span}\{\varphi_j\}_{j=1}^r$. Next, we develop the POD reduced order model of the heat equation by substituting u_r for the unknown u, using the Galerkin method, and projecting Equation (30) onto the space $V_r^h \subset V^h$. Thus we arrive at the following backward Euler POD reduced order model (BE-POD-ROM):

$$\left(\frac{u_r^{n+1} - u_r^n}{\Delta t}, v_r\right)_{L^2} + \nu(\nabla u_r^{n+1}, \nabla v_r)_{L^2} = (f^{n+1}, v_r)_{L^2} \quad \forall v_r \in V_r^h. \tag{31}$$

We split the error, in the standard way, with

$$e^{n+1} = u^{n+1} - u_r^{n+1} = (u^{n+1} - R_r u^{n+1}) - (u_r^{n+1} - R_r u^{n+1}) = \eta^{n+1} - \phi_r^{n+1}$$

where R_r is a projection onto V_r^h, $\eta^{n+1} = u^{n+1} - R_r u^{n+1}$ is the POD projection error, and $\phi_r^{n+1} = u_r^{n+1} - R_r u^{n+1}$ is the discretization error. We subtract Equation (31) from Equation (30) with test function $v = v_r$ and make the error substitution given above to get

$$\begin{aligned} &\left(\frac{\phi_r^{n+1} - \phi_r^n}{\Delta t}, v_r\right)_{L^2} + \nu(\nabla \phi_r^{n+1}, \nabla v_r)_{L^2} \\ &= \left(\frac{\eta^{n+1} - \eta^n}{\Delta t}, v_r\right)_{L^2} + \nu(\nabla \eta^{n+1}, \nabla v_r)_{L^2} \quad \forall v_r \in V_r^h. \end{aligned} \tag{32}$$

Remark 2 The approach taken in this work is different than the one taken in [29]. In that work the authors compare the ROM solution u_r^n to the exact solution of the

PDE $u(t_n)$. We can bound the error between the ROM solution and the exact solution using the triangle inequality

$$\|u_r^n - u(t_n)\|_Y \leq \|u_r^n - u^n\|_Y + \|u^n - u(t_n)\|_Y$$

where Y is a Hilbert space. The current work focuses on bounding the ROM error term $\|u_r^n - u^n\|_Y$ with $Y = L^2(\Omega)$ or $Y = H_0^1(\Omega)$ and leaves the second term to be studied using well-known finite element theory.

Remark 3 For analysis and computations the initial condition is taken to be the POD projection of the given initial condition, i.e., $u_r^1 = \Pi_r^X u^1$. Other initial conditions are possible and have been considered in other works for the standard POD and DQ POD approaches. For example, in [29], the Ritz projection was used for the initial condition. We discuss the choice of initial condition and the impact on the error analysis in Section 4.3.

We now consider each POD space, $L^2(\Omega)$ and $H_0^1(\Omega)$, separately.

4.1 POD space: $L^2(\Omega)$

In this section, we take X to be the space $L^2(\Omega)$. The orthogonal projection onto V_r^h, $\Pi_r^X : L^2(\Omega) \to L^2(\Omega)$, is given by

$$\Pi_r^X u = \sum_{i=1}^{r} (u, \varphi_i)_{L^2} \varphi_i \tag{33}$$

and the set of POD modes $\{\varphi_i\}$ are orthonormal in $L^2(\Omega)$. Define R_r to be the Ritz projection which satisfies

$$(\nabla(w - R_r w), \nabla v_r)_{L^2} = 0 \tag{34}$$

for all $v_r \in V_r^h$. Thus, for all $w \in V^h$ we have

$$\|w - R_r w\|_{H_0^1} = \inf_{v_r \in V_r^h} \|w - v_r\|_{H_0^1}.$$

Let $\eta_{Ritz}^{n+1} = u^{n+1} - R_r u^{n+1}$. Then, Equation (32) becomes

$$\left(\frac{\phi_r^{n+1} - \phi_r^n}{\Delta t}, v_r\right)_{L^2} + \nu(\nabla \phi_r^{n+1}, \nabla v_r)_{L^2} = \left(\frac{\eta_{Ritz}^{n+1} - \eta_{Ritz}^n}{\Delta t}, v_r\right)_{L^2} \quad \forall v_r \in V_r^h. \tag{35}$$

Using this ROM error equation, we obtain the error bounds given below. Note, the constant C can change from step to step, but it does not depend on any discretization parameter. In Section 5.3, we investigate the final value of C computationally.

Theorem 9 *The pointwise $L^2(\Omega)$ solution error when the $L^2(\Omega)$ POD basis is used for the BE-POD-ROM is bounded by*

$$\max_k \|e^k\|_{L^2}^2 \leq C\left(\sum_{i=r+1}^{s} \lambda_i^{DQ1}\|\varphi_i - R_r\varphi_i\|_{L^2}^2 + \|\phi_r^1\|_{L^2}^2\right). \tag{36}$$

Proof Taking $v_r = \phi_r^{n+1}$ in Equation (35) yields

$$\left(\frac{\phi_r^{n+1}-\phi_r^n}{\Delta t}, \phi_r^{n+1}\right)_{L^2} + \nu\|\nabla\phi_r^{n+1}\|_{L^2}^2 = \left(\frac{\eta_{Ritz}^{n+1}-\eta_{Ritz}^n}{\Delta t}, \phi_r^{n+1}\right)_{L^2}. \tag{37}$$

Now, apply Cauchy-Schwarz followed by Young's inequality with a constant δ to get

$$\left(\frac{\phi_r^{n+1}-\phi_r^n}{\Delta t}, \phi_r^{n+1}\right)_{L^2} + \nu\|\nabla\phi_r^{n+1}\|_{L^2}^2 \leq \frac{1}{4\delta}\|\partial\eta_{Ritz}^n\|_{L^2}^2 + \delta\|\phi_r^{n+1}\|_{L^2}^2. \tag{38}$$

Finally, apply a polarization identity, use the fact that $C\|\phi_r^{n+1}\|_{L^2}^2 \leq \|\nabla\phi_r^{n+1}\|_{L^2}^2$, and rearrange to obtain

$$\left(\frac{1}{2\Delta t} - \delta + \nu C\right)\|\phi_r^{n+1}\|_{L^2}^2 - \frac{1}{2\Delta t}\|\phi_r^n\|_{L^2}^2 \leq \frac{1}{4\delta}\|\partial\eta_{Ritz}^n\|_{L^2}^2. \tag{39}$$

Taking $\delta = \nu C$ and multiplying by $2\Delta t$ we get

$$\|\phi_r^{n+1}\|_{L^2}^2 - \|\phi_r^n\|_{L^2}^2 \leq \frac{\Delta t}{2\nu C}\|\partial\eta_{Ritz}^n\|_{L^2}^2. \tag{40}$$

Summing from $n = 1$ to $n = k-1$, using $e^n = \eta_{Ritz}^n - \phi_r^n$ and $(a-b)^2 \leq 2(a^2+b^2)$ to give $\|e^n\|_{L^2}^2 \leq 2(\|\eta_{Ritz}^n\|_{L^2}^2 + \|\phi_r^n\|_{L^2}^2)$, and rearranging once again gives

$$\|e^k\|_{L^2}^2 \leq C\left(\Delta t\sum_{n=1}^{k-1}\|\partial\eta_{Ritz}^n\|_{L^2}^2 + \|\eta_{Ritz}^k\|_{L^2}^2 + \|\phi_r^1\|_{L^2}^2\right). \tag{41}$$

Then, apply Lemma 5 and Theorem 7 with $Y = L^2(\Omega)$ and $\pi_r = R_r$ to get

$$\|e^k\|_{L^2}^2 \leq C\left(\sum_{i=r+1}^{s} \lambda_i^{DQ1}\|\varphi_i - R_r\varphi_i\|_{L^2}^2 + \|\phi_r^1\|_{L^2}^2\right). \tag{42}$$

Take the maximum over all k to get the result. □

Theorem 10 *The pointwise $H_0^1(\Omega)$ solution error when the $L^2(\Omega)$ POD basis is used for the BE-POD-ROM is bounded by*

$$\begin{aligned}&\max_k \|\nabla e^k\|_{L^2}^2 \\ &\leq C\left(\sum_{i=r+1}^{s} \lambda_i^{DQ1}\left(\|\varphi_i - R_r\varphi_i\|_{L^2}^2 + \|\nabla(\varphi_i - R_r\varphi_i)\|_{L^2}^2\right) + \|\phi_r^1\|_{H_0^1}^2\right).\end{aligned} \tag{43}$$

Proof Taking $v_r = \partial\phi_r^n$ in Equation (35) gives

$$\left(\frac{\phi_r^{n+1}-\phi_r^n}{\Delta t}, \partial\phi_r^n\right)_{L^2} + \nu\left(\nabla\phi_r^{n+1}, \nabla\partial\phi_r^n\right)_{L^2} = \left(\frac{\eta_{Ritz}^{n+1}-\eta_{Ritz}^n}{\Delta t}, \partial\phi_r^n\right)_{L^2}. \quad (44)$$

Rearranging and using the definition of $\partial\phi_r^n$ yields

$$\nu\left(\nabla\phi_r^{n+1}, \nabla\partial\phi_r^n\right)_{L^2} = \left(\frac{\eta_{Ritz}^{n+1}-\eta_{Ritz}^n}{\Delta t}, \partial\phi_r^n\right)_{L^2} - \|\partial\phi_r^n\|_{L^2}^2. \quad (45)$$

Then, applying first the Cauchy-Schwarz inequality followed by Young's inequality with the constant δ we obtain

$$\begin{aligned}\nu\left(\nabla\phi_r^{n+1}, \nabla\partial\phi_r^n\right)_{L^2} &\le \left(\|\partial\eta_{Ritz}^n\|_{L^2}\|\partial\phi_r^n\|_{L^2}\right) - \|\partial\phi_r^n\|_{L^2}^2 \\ &\le \left(\frac{1}{4\delta}\|\partial\eta_{Ritz}^n\|_{L^2}^2 + \delta\|\partial\phi_r^n\|_{L^2}^2\right) - \|\partial\phi_r^n\|_{L^2}^2 \\ &= \frac{1}{4\delta}\|\partial\eta_{Ritz}^n\|_{L^2}^2 + (\delta-1)\|\partial\phi_r^n\|_{L^2}^2.\end{aligned}$$

Taking the constant $\delta = 1$ yields

$$\nu\left(\nabla\phi_r^{n+1}, \nabla\partial\phi_r^n\right)_{L^2} \le \frac{1}{4}\|\partial\eta_{Ritz}^n\|_{L^2}^2. \quad (46)$$

Also, using a polarization identity

$$\Delta t\left(\nabla\phi_r^{n+1}, \nabla\partial\phi_r^n\right)_{L^2} = \frac{1}{2}\left(\|\nabla\phi_r^{n+1}\|_{L^2}^2 + \|\nabla\phi_r^{n+1}-\nabla\phi_r^n\|_{L^2}^2 - \|\nabla\phi_r^n\|_{L^2}^2\right). \quad (47)$$

Combining Equation (46) and Equation (47), summing over $n = 1, \ldots, k-1$, and using $\|\nabla e^k\|_{L^2}^2 \le 2\left(\|\nabla\eta_{Ritz}^k\|_{L^2}^2 + \|\nabla\phi_r^k\|_{L^2}^2\right)$ gives

$$\|\nabla e^k\|_{L^2}^2 \le C\left(\Delta t\sum_{n=1}^{k-1}\|\partial\eta_{Ritz}^n\|_{L^2}^2 + \|\eta_{Ritz}^k\|_{H_0^1}^2 + \|\phi_r^1\|_{H_0^1}^2\right). \quad (48)$$

Then, apply Lemma 5 and Theorem 7 with $Y = H_0^1(\Omega)$ and $\pi_r = R_r$ to get

$$\begin{aligned}&\|\nabla e^k\|_{L^2}^2 \\ &\le C\left(\sum_{i=r+1}^{s}\lambda_i^{DQ1}\|\varphi_i - R_r\varphi_i\|_{L^2}^2 + \sum_{i=r+1}^{s}\lambda_i^{DQ1}\|\varphi_i - R_r\varphi_i\|_{H_0^1}^2 + \|\phi_r^1\|_{H_0^1}^2\right). \quad (49)\end{aligned}$$

Rearrange and take the maximum over all k to get the result. □

Theorem 11 *The pointwise solution norm error when the $L^2(\Omega)$ POD basis is used for the BE-POD-ROM is bounded by*

$$\| e^N \|_{L^2}^2 + \nu \Delta t \sum_{n=1}^{N-1} \|\nabla e^{n+1}\|_{L^2}^2 \leq C \left(\sum_{i=r+1}^{s} \lambda^{DQ1} (\|\varphi_i - R_r \varphi_i\|_{L^2}^2 + \|\varphi_i - R_r \varphi_i\|_{H_0^1}^2) + \|\phi_r^1\|_{L^2}^2 \right). \quad (50)$$

Proof Taking ϕ_r^{n+1} in Equation (35), yields

$$\left(\frac{\phi_r^{n+1} - \phi_r^n}{\Delta t}, \phi_r^{n+1} \right)_{L^2} + \nu \|\nabla \phi_r^{n+1}\|_{L^2}^2 = \left(\frac{\eta_{Ritz}^{n+1} - \eta_{Ritz}^n}{\Delta t}, \phi_r^{n+1} \right)_{L^2}. \quad (51)$$

Now, apply the Cauchy-Schwarz inequality, Young's inequality, and a polarization identity to get

$$\frac{1}{2\Delta t} \left(\|\phi_r^{n+1}\|_{L^2}^2 - \|\phi_r^n\|_{L^2}^2 \right) + \nu \|\nabla \phi_r^{n+1}\|_{L^2}^2 \leq \frac{1}{4\delta} \|\partial \eta_{Ritz}^n\|_{L^2}^2 + \delta \|\phi_r^{n+1}\|_{L^2}^2. \quad (52)$$

Now. multiply by 2, apply the Poincaré inequality to the last term, and combine the resulting terms:

$$\frac{1}{\Delta t} \left(\|\phi_r^{n+1}\|_{L^2}^2 - \|\phi_r^n\|_{L^2}^2 \right) + 2 \left(\nu - \frac{\delta}{C} \right) \|\nabla \phi_r^{n+1}\|_{L^2}^2 \leq \frac{1}{2\delta} \|\partial \eta_{Ritz}^n\|_{L^2}^2. \quad (53)$$

Take $\delta = \frac{\nu C}{2}$ and multiply by Δt:

$$\|\phi_r^{n+1}\|_{L^2}^2 - \|\phi_r^n\|_{L^2}^2 + \nu \Delta t \|\nabla \phi_r^{n+1}\|_{L^2}^2 \leq \frac{\Delta t}{\nu C} \|\partial \eta_{Ritz}^n\|_{L^2}^2. \quad (54)$$

Sum from $n = 1$ to $k - 1$, rearrange, and take a maximum amoung the constants to obtain

$$\|\phi_r^k\|_{L^2}^2 + \nu \Delta t \sum_{n=1}^{k-1} \|\nabla \phi_r^{n+1}\|_{L^2}^2 \leq C \left(\Delta t \sum_{n=1}^{k-1} \|\partial \eta_{Ritz}^n\|_{L^2}^2 + \|\phi_r^1\|_{L^2}^2 \right). \quad (55)$$

Using $\|e^n\|_{L^2}^2 \leq 2(\|\eta_{Ritz}^n\|_{L^2}^2 + \|\phi_r^n\|_{L^2}^2)$ and rearranging gives

$$\| e^k \|_{L^2}^2 + \nu \Delta t \sum_{n=1}^{k-1} \|e^{n+1}\|_{H_0^1}^2 \leq C \left(\Delta t \sum_{n=1}^{k-1} \|\partial \eta_{Ritz}^n\|_{L^2}^2 + \|\eta_{Ritz}^k\|_{L^2}^2 + \Delta t \sum_{n=1}^{k-1} \|\eta_{Ritz}^{n+1}\|_{H_0^1}^2 + \|\phi_r^1\|_{L^2}^2 \right). \quad (56)$$

Finally, using Lemma 5, Theorem 7, and Corollary 8 with $\pi_r = R_r$ and both $Y = L^2(\Omega)$ and $Y = H_0^1(\Omega)$ yield

$$\| e^k \|_{L^2}^2 + \nu \Delta t \sum_{n=1}^{k-1} \| e^{n+1} \|_{H_0^1}^2 \leq C \left(\sum_{i=r+1}^{s} \lambda^{DQ1} (\| \varphi_i - R_r \varphi_i \|_{L^2}^2 + \| \varphi_i - R_r \varphi_i \|_{H_0^1}^2) + \| \phi_r^1 \|_{L^2}^2 \right). \quad (57)$$

Taking $k = N$ yields the result. □

4.2 POD space: $H_0^1(\Omega)$

Alternatively, we can take the POD space X to be $H_0^1(\Omega)$. The orthogonal projection onto V_r^h, $\Pi_r^X : H_0^1(\Omega) \to H_0^1(\Omega)$, is given by

$$\Pi_r^X u = \sum_{i=1}^{r} (u, \varphi_i)_{H_0^1} \varphi_i \quad (58)$$

and the set of POD modes $\{\varphi_i\}$ are orthonormal in $H_0^1(\Omega)$.

Note that $\Pi_r^X \varphi_k = \sum_{i=1}^{r} (\varphi_k, \varphi_i)_{H_0^1} \varphi_i = 0$ for $k > r$ since $\{\varphi_k\}$ are orthogonal in $H_0^1(\Omega)$. Furthermore, since Π_r^X is orthogonal we have

$$\begin{aligned} & (w - \Pi_r^X w, v_r)_X = 0 \quad \forall v_r \in V_r^h \\ \Longrightarrow \quad & (w - \Pi_r^X w, v_r)_{H_0^1} = 0 \quad \forall v_r \in V_r^h \\ \Longrightarrow \quad & (\nabla (w - \Pi_r^X w), \nabla v_r)_{L^2} = 0 \quad \forall v_r \in V_r^h. \end{aligned}$$

Similar to before, we take R_r to be the Ritz projection, but in this case the Ritz projection is the orthogonal projection Π_r^X, and Equation (32) becomes

$$\left(\frac{\phi_r^{n+1} - \phi_r^n}{\Delta t}, v_r \right)_{L^2} + \nu (\nabla \phi_r^{n+1}, \nabla v_r)_{L^2} = \left(\frac{\eta_{Ritz}^{n+1} - \eta_{Ritz}^n}{\Delta t}, v_r \right)_{L^2} \quad \forall v_r \in V_r^h \quad (59)$$

where $\eta_{Ritz}^{n+1} = u^{n+1} - R_r u^{n+1} = u^{n+1} - \Pi_r^X u^{n+1}$. As before we can show error bounds for the $L^2(\Omega)$ and $H_0^1(\Omega)$ norm errors and the solution norm error.

Theorem 12 *The pointwise ROM solution errors when the $H_0^1(\Omega)$ POD basis is used for the BE-POD-ROM are bounded as follows:*

$$\max_k \| e^k \|_{L^2}^2 \leq C \left(\sum_{i=r+1}^{s} \lambda_i^{DQ1} \| \varphi_i \|_{L^2}^2 + \| \phi_r^1 \|_{L^2}^2 \right), \quad (60)$$

$$\max_k \| \nabla e^k \|_{L^2}^2 \leq C \left(\sum_{i=r+1}^{s} \lambda_i^{DQ1} (\| \varphi_i \|_{L^2}^2 + 1) + \| \phi_r^1 \|_{H_0^1}^2 \right), \quad (61)$$

and

$$\|e^N\|_{L^2}^2 + \nu\Delta t \sum_{n=1}^{N-1} \|\nabla e^{n+1}\|_{L^2}^2 \leq C \left(\sum_{i=r+1}^{s} \lambda^{DQ1}(1 + \|\varphi_i\|_{L^2}^2) + \|\phi_r^1\|_{L^2}^2 \right). \quad (62)$$

Proof Proceed as in the proofs of Theorem 9, Theorem 10, and Theorem 11 respectively, but now use $\eta_{Ritz} = u - \Pi_r^X u$ and the appropriate choices for Y in Theorem 7, Corollary 8, and Lemma 5. □

4.3 Optimality

In this section, we investigate the optimality of this new approach to POD with difference quotients. To do so, we follow the approach given in [29] but modify the optimality definitions given there to include the ROM error for the initial condition. For this work, we focus on the POD ROM discretization errors for both the PDE and the initial condition, and assume the time and spatial discretization errors are optimal. Thus, we ignore the latter errors in the equation given below. In this section, we consider only the new approach as the standard difference quotient approach is discussed in [29]. The optimality of each error depends on both the POD space X and the error norm space Y. To give a precise definition of pointwise ROM error optimality, assume there exists a constant $C > 0$ that is independent of the discretization parameters such that the ROM errors $e^k = u^k - u_r^k$ for $k = 1, \ldots, N$ satisfy

$$\max_{1 \leq k \leq N} \|e^k\|_Y^2 \leq C \left(\Lambda_r + \Lambda_r^1 \right) \quad (63)$$

where

- Λ_r is the ROM discretization error for the PDE, which depends only on r, the POD eigenvalues, and the POD modes;
- Λ_r^1 is the ROM discretization error for the initial condition, which depends only on r, the POD eigenvalues, and the POD modes.

As mentioned in Remark 3, in [29] the initial condition for the ROM was chosen to be the Ritz projection of the actual initial condition, i.e., $u_r^1 = R_r u^1$. This leads to zero ROM discretization error for the initial condition, i.e., $\Lambda_r^1 = 0$, since $\phi_r^1 = u_r^1 - R_r u^1$, where u_r^1 is the initial condition for the ROM. In this work, we use the POD projection for the initial condition, i.e., $u_r^1 = \Pi_r^X u^1$, since this is another very common choice for the initial condition in the literature. This choice gives $\Lambda_r^1 \neq 0$, and below we show that this can impact the optimality of the ROM discretization errors.

Let $X_r \subset X$ be the span of the first r POD modes, and assume $X_r \subset Y$. Let $\Pi_r^X : X \to X$ be the orthogonal projection onto X_r and $\Pi_r^Y : Y \to Y$ be the $Y-$orthogonal projection onto X_r. Furthermore, let s be the number of positive POD eigenvalues. In Definition 1, we extend the definitions of optimality provided in [29] to include the ROM discretization error for the initial condition.

Definition 1 We say the total ROM discretization error, $\Lambda_r + \Lambda_r^1$, is

- **optimal-I** if there exists a constant C such that

$$\Lambda_r + \Lambda_r^1 \leq C \sum_{i=r+1}^{s} \lambda_i \|\varphi_i\|_Y^2, \tag{64}$$

- **optimal-II** if there exists a constant C such that

$$\Lambda_r + \Lambda_r^1 \leq C \sum_{i=r+1}^{s} \lambda_i \|\varphi_i - \Pi_r^Y \varphi_i\|_Y^2. \tag{65}$$

The constant C can depend on the solution data and the problem data, but does not depend on any discretization parameter.

Remark 4 For a detailed discussion on the optimality types, see [29]. Note that, as shown in [29, Proposition 4.8], optimal-II is stronger than optimal-I, and the two are equivalent if $X = Y$.

First, we consider the ROM error from the choice of initial condition by noting $\Lambda_r^1 = \|\phi_r^1\|_Y^2$ in Lemma 13 below. Throughout this section, we use R_r to denote the Ritz projection.

Lemma 13 *Let the initial condition be the POD projection of the given initial condition, i.e.,* $u_r^1 = \Pi_r^X u^1$ *so that* $\phi_r^1 = u_r^1 - R_r u^1 = \Pi_r^X u^1 - R_r u^1$. *If* $X = L^2(\Omega)$, *then*

$$\|\phi_r^1\|_{L^2}^2 \leq 2 \sum_{i=r+1}^{s} \lambda_i + 2 \sum_{i=r+1}^{s} \lambda_i \|\varphi_i - R_r \varphi_i\|_{L^2}^2 \tag{66}$$

and

$$\|\phi_r^1\|_{H_0^1}^2 \leq 2 \sum_{i=r+1}^{s} \lambda_i \|\varphi_i\|_{H_0^1}^2 + 2 \sum_{i=r+1}^{s} \lambda_i \|\varphi_i - R_r \varphi_i\|_{H_0^1}^2. \tag{67}$$

If $X = H_0^1(\Omega)$, *then*

$$\phi_r^1 = 0 \tag{68}$$

for either choice of space Y.

Proof First, consider the case $X = L^2(\Omega)$. We have

$$\begin{aligned} \|\phi_r^1\|_Y^2 &= \|u_r^1 - R_r u^1\|_Y^2 \\ &= \|\Pi_r^X u^1 - R_r u^1\|_Y^2 \\ &\leq 2\|\Pi_r^X u^1 - u^1\|_Y^2 + 2\|u^1 - R_r u^1\|_Y^2. \end{aligned}$$

Using Lemma 5 with $Y = X = L^2(\Omega)$ and $\pi_r = R_r$ gives Equation (66) and with $Y = H_0^1(\Omega)$ and $\pi_r = R_r$ gives Equation (67). Finally, if $X = H_0^1(\Omega)$, then $\Pi_r^X = R_r$ and Equation (68) follows by definition of π_r. □

This lemma allows us to investigate the total ROM discretization error in the following two theorems with the POD space taken to be L^2 and H_0^1 respectively. Note, as before, in the statement and proof of the following theorem the constant C might change from line to line.

Theorem 14 *If the L^2 POD basis is used, i.e., $X = L^2(\Omega)$, then the following hold:*

- *The pointwise ROM error in* Equation (36) *with the error norm $Y = L^2$ is optimal-I if there exists a constant C such that*

$$\|\varphi_i - R_r\varphi_i\|_{L^2} \leq C \tag{69}$$

  for $r+1 \leq i \leq s$. Note that in this case optimal-I is equivalent to optimal-II.
- *The pointwise ROM error in* Equation (43) *with error norm $Y = H_0^1(\Omega)$ is optimal-I.*

Remark 5 In [29, Theorem 4.10 (iv)], when using the L^2 POD basis with $Y = H_0^1(\Omega)$ but not considering the initial condition error the ROM error was optimal-II. When including the initial condition as the POD projection of the given initial condition, we obtain the weaker result that the error is optimal-I. Other choices of initial condition will yield different results. Furthermore, the assumption Equation (69) is discussed in greater detail in [29, Section 4.2].

Proof For the first item

$$\begin{aligned}
\Lambda_r + \Lambda_r^1 &= \sum_{i=r+1}^{s} \lambda_i \|\varphi_i - R_r\varphi_i\|_{L^2}^2 + \|\phi_r^1\|_{L^2}^2 \\
&\leq \sum_{i=r+1}^{s} \lambda_i \|\varphi_i - R_r\varphi_i\|_{L^2}^2 + 2\left(\sum_{i=r+1}^{s} \lambda_i + \sum_{i=r+1}^{s} \lambda_i \|\varphi_i - R_r\varphi_i\|_{L^2}^2\right) \\
&\leq C \sum_{i=r+1}^{s} \lambda_i \\
&= C \sum_{i=r+1}^{s} \lambda_i \|\varphi_i\|_{L^2}^2
\end{aligned}$$

using Lemma 13, the assumption in Equation (69), Theorem 7, and the L^2 orthonormality of the POD basis.

For the second item, use the Poincaré inequality to get

$$\begin{aligned}
\Lambda_r + \Lambda_r^1 &= \sum_{i=r+1}^{s} \lambda_i \|\varphi_i - R_r\varphi_i\|_{L^2}^2 + \sum_{i=r+1}^{s} \lambda_i \|\nabla(\varphi_i - R_r\varphi_i)\|_{L^2}^2 + \|\phi_r^1\|_{H_0^1}^2 \\
&\leq C \sum_{i=r+1}^{s} \lambda_i \|\varphi_i - R_r\varphi_i\|_{H_0^1}^2 + \|\phi_r^1\|_{H_0^1}^2.
\end{aligned}$$

Lemma 13 and the orthogonality of the Ritz projection $R_r : H_0^1(\Omega) \to H_0^1(\Omega)$ then yields

$$\Lambda_r + \Lambda_r^1 \leq C \sum_{i=r+1}^{s} \lambda_i \|\varphi_i - R_r\varphi_i\|_{H_0^1}^2 + C \sum_{i=r+1}^{s} \lambda_i \|\varphi_i\|_{H_0^1}^2 \leq C \sum_{i=r+1}^{s} \lambda_i \|\varphi_i\|_{H_0^1}^2.$$

Thus, the error given in Equation (43) is optimal-I. □

Theorem 15 *If the $H_0^1(\Omega)$ POD basis is used, i.e., $X = H_0^1$, then the following results hold.*

- *The pointwise ROM error in* Equation (60) *with the error norm $Y = L^2(\Omega)$ is optimal-I.*
- *The pointwise ROM error in* Equation (60) *with error norm $Y = L^2(\Omega)$ is also optimal-II when*

$$\|\varphi_i\|_Y \leq C\|\varphi_i - \Pi_r^Y \varphi_i\|_Y \quad \text{for } r+1 \leq i \leq s.$$

- *The pointwise ROM error in* Equation (61) *with the error norm $Y = H_0^1(\Omega)$ is optimal-I. Note that in this case optimal-I is equivalent to optimal-II.*

The proof of this result is similar to that of [29, Theorem 4.10] since from Lemma 13 we know $\phi_r^1 = 0$ for both $Y = L^2(\Omega)$ and $Y = H_0^1(\Omega)$. We omit the details. We note that the optimality results for the new POD DQ approach in Theorems 14 and 15 are very similar to [29, Theorem 4.10] for the standard POD DQ approach. In fact, the only fundamental difference in the results here was caused by our choice of the initial condition and including this in the optimality definition, as discussed in Remark 5.

5 Numerical results

We now turn our attention to computational results. In this section we use the same test problem as in Section 3.1 to compute ROM solution errors in order to compare the new POD approach to the existing standard approaches. We also compute the scaling factors present in the bounds of the theoretical results from Theorem 7 and Section 4.

5.1 ROM comparisons for the three POD approaches

First, we report the computed ROM errors for the new POD DQ approach at the final time, i.e., the errors at $T = 1$. Note that this corresponds to the case where $k = N$, and we are not taking the maximum. We compute both the $L^2(\Omega)$ norm error and the $H_0^1(\Omega)$ norm error. For this computation, we use 100 finite element nodes, 100 time steps and 3 different values for r. Note that for the final time errors here in Section 5.1 we report the errors and not the norm square errors that are presented in later sections. The solution norm error is a norm squared error. For comparison we also show the final time errors for the standard POD approach and the standard DQ POD approach.

Table 2 ROM errors for the L^2 norm at the final time: $\|e_r^N\|_{L^2} = \|u^N - u_r^N\|_{L^2}$

POD space	r value	Standard POD	Standard DQ POD	New DQ POD
L^2	4	1.639e–08	1.206e–07	1.141e–07
	6	1.257e–10	1.148e–09	1.090e–09
	8	9.486e–13	9.144e–12	8.722e–12
H_0^1	4	1.851e–08	1.350e–07	1.276e–07
	6	1.324e–10	1.218e–09	1.156e–09
	8	9.999e–13	9.778e–12	9.323e–12

First, we consider the case where the POD space is taken to be $X = L^2(\Omega)$. The results for the $L^2(\Omega)$ and $H_0^1(\Omega)$ errors can be found in Tables 2 and 3 respectively. In Table 4, we compute the solution norm squared errors for this reduced order model using the same computation parameters. This solution norm error at the final time is given by Equation (70):

$$\|e^N\|_{L^2}^2 + \Delta t \sum_{n=1}^{N-1} \|\nabla e^{n+1}\|_{L^2}^2. \tag{70}$$

We also wish to compare the different POD approaches when we take the POD space to be $H_0^1(\Omega)$, i.e., $X = H_0^1(\Omega)$. All other parameters of the computation stay the same and the results can also be found in Tables 2, 3, and 4. For both cases of the chosen POD space the errors behave similarly in all three approaches but are particularly close in the two approaches that utilize the difference quotients.

For this example, note that the standard POD errors are one order of magnitude smaller than both types of POD DQ errors. The magnitude difference of the errors is likely related to the magnitude differences of the POD singular values for all three approaches discussed in Section 3.1. A thorough investigation of the magnitudes of the errors for the different POD approaches for different PDEs is very important, but we leave this to be considered elsewhere.

Table 3 ROM errors for the H_0^1 norm at the final time: $\|e_r^N\|_{H_0^1} = \|u^N - u_r^N\|_{H_0^1}$

POD space	r value	Standard POD	Standard DQ POD	New DQ POD
L^2	4	1.936e–07	1.340e–06	1.269e–06
	6	2.615e–09	2.364e–08	2.245e–08
	8	2.264e–11	2.123e–10	2.024e–10
H_0^1	4	2.171e–07	1.494e–06	1.413e–06
	6	2.755e–09	2.506e–08	2.379e–08
	8	2.396e–11	2.263e–10	2.157e–10

Table 4 ROM solution norm error Equation (70)

POD Space	r value	Standard POD	Standard DQ POD	New DQ POD
L^2	4	1.172e–07	2.441e–06	2.008e–06
	6	1.472e–11	4.373e–10	3.576e–10
	8	7.032e–16	2.227e–14	1.810e–14
H_0^1	4	1.135e–07	3.049e–06	2.525e–06
	6	1.467e–11	4.861e–10	3.996e–10
	8	6.984e–16	2.479e–14	2.032e–14

5.2 Pointwise POD projection error bounds

We compute the ratios generated by the theoretical results concerning the pointwise POD projection errors in Section 3.2. For these results, we vary the number of time steps, while keeping everything else constant. This allows us to verify that the scaling factors are not dependent on the time step chosen. We performed similar experiments by varying other parameters and obtained similar results. We use 100 finite element nodes and choose $r = 4$. Both $X = L^2(\Omega)$ and $X = H_0^1(\Omega)$ are considered in this section. We use the data generated by the finite element method as described in Section 3.1 and compute the POD modes and POD singular values.

First, we consider the pointwise error bounds as in Theorem 7. The tables show the projection and the norm space Y that is used for each of the computations. Note that for these we have $\pi_r = R_r$ and either $Y = L^2(\Omega)$ or $Y = H_0^1(\Omega)$. For example, for the second result in Theorem 7 with $X = L^2(\Omega)$ and $Y = H_0^1(\Omega)$ we have

$$\text{scaling factor} = \left(\max_j \|u^j - \Pi_r^X u^j\|_Y^2 \right) / \left(\sum_{i=r+1}^{s} \lambda_i^{DQ1} \|\varphi_i\|_Y^2 \right).$$

The results for $X = L^2(\Omega)$ and $X = H_0^1(\Omega)$ are given in Tables 5 and 6 respectively. Theoretically, we showed that the scaling factor should always be less that or equal to 2 (since $T = 1$ here). The computational results show that the scaling factor can be much less than that value.

Table 5 Scaling factors for Theorem 7 as Δt changes with $X = L^2(\Omega)$

Projection	Y	1/40	1/50	1/100	1/200	1/300
Π_r^X	$L^2(\Omega)$	6.0e–02	5.4e–02	4.0e–02	3.2e–02	2.9e–02
Π_r^X	$H_0^1(\Omega)$	5.6e–02	4.9e–02	3.3e–02	2.3e–02	1.8e–02
R_r	$L^2(\Omega)$	5.8e–02	5.2e–02	3.7e–02	2.9e–02	2.5e–02
R_r	$H_0^1(\Omega)$	5.5e–02	4.9e–02	3.2e–02	2.1e–02	1.6e–02

Table 6 Scaling factors for Theorem 7 as Δt changes with $X = H_0^1(\Omega)$

Projection	Y	1/40	1/50	1/100	1/200	1/300
Π_r^X	$L^2(\Omega)$	6.5e–02	5.8e–02	4.2e–02	3.1e–02	2.6e–02
Π_r^X	$H_0^1(\Omega)$	6.8e–02	6.2e–02	4.8e–02	4.0e–02	3.6e–02
R_r	$L^2(\Omega)$	6.5e–02	5.9e–02	4.3e–02	3.3e–02	2.8e–02
R_r	$H_0^1(\Omega)$	7.0e–02	6.4e–02	5.1e–02	4.4e–02	4.1e–02

5.3 ROM error bounds

Next, we consider the reduced order model error bounds from Section 4. Again, we use 100 finite element nodes and $r = 4$ with varying values of Δt. First, define the following values:

$$\text{err}_1 = \max_k \|e^k\|_{L^2}^2,$$

$$\text{err}_2 = \max_k \|e^k\|_{H_0^1}^2,$$

and

$$\text{err}_3 = \|e^N\|_{L^2}^2 + \Delta t \sum_{n=1}^{N-1} \|\nabla e^{n+1}\|_{L^2}^2.$$

For the first set of scaling factors defined in Equation (71), Equation (72), and Equation (73) below, we have $X = L^2(\Omega)$. These equations correspond to Equation (36) from Theorem 9, Equation 43 from Theorem 10, and Equation (50) from Theorem 11 respectively. We also compute the scaling factors for the results that use $X = H_0^1(\Omega)$ as the POD space. These scaling factors for the $X = H_0^1(\Omega)$ case are given by Equation (74) to (76). These equations correspond to Equations (60) to (62) from Theorem 12. For these computations, we once again vary the time steps and keep all other parameters constant. The results for both cases of POD basis space can be found in Table 7.

$$C_1 = \text{err}_1 / \left(\sum_{i=r+1}^{s} \lambda_i^{DQ1} \|\varphi_i - R_r\varphi_i\|_{L^2}^2 + \|\phi_r^1\|_{L^2}^2 \right) \tag{71}$$

$$C_2 = \text{err}_2 / \left(\sum_{i=r+1}^{s} \lambda_i^{DQ1} \left(\|\varphi_i - R_r\varphi_i\|_{L^2}^2 + \|\nabla(\varphi_i - R_r\varphi_i)\|_{L^2}^2 \right) + \|\phi_r^1\|_{H_0^1}^2 \right) \tag{72}$$

$$C_3 = \text{err}_3 / \left(\sum_{i=r+1}^{s} \lambda^{DQ1} (\|\varphi_i - R_r\varphi_i\|_{L^2}^2 + \|\nabla(\varphi_i - R_r\varphi_i)\|_{L^2}^2) + \|\phi_r^1\|_{L^2}^2 \right) \tag{73}$$

$$C_4 = \text{err}_1 / \left(\sum_{i=r+1}^{s} \lambda_i^{DQ1} \|\varphi_i\|_{L^2}^2 + \|\phi_r^1\|_{L^2}^2 \right) \tag{74}$$

Table 7 Scaling factors as Δt changes for ROM errors

Δt	1/40	1/50	1/100	1/200	1/300
C_1	5.8e–02	5.1e–02	3.7e–02	2.8e–02	2.5e–02
C_2	1.0e–05	1.4e–05	2.9e–05	4.0e–05	4.3e–05
C_3	1.9e–06	2.4e–06	4.1e–05	5.2e–06	5.3e–06
C_4	6.7e–02	6.1–e02	4.7e–02	4.0e–02	3.6e–02
C_5	6.5e–02	5.8e–02	4.1e–02	3.0e–02	2.6e–02
C_6	1.1e–02	9.3e–03	5.7e–03	3.8e–03	3.1e–03

$$C_5 = \mathrm{err}_2 / \left(\sum_{i=r+1}^{s} \lambda_i^{DQ1} (\|\varphi_i\|_{L^2}^2 + 1) + \|\phi_r^1\|_{H_0^1}^2 \right) \tag{75}$$

$$C_6 = \mathrm{err}_3 / \left(\sum_{i=r+1}^{s} \lambda_i^{DQ1} (1 + \|\varphi_i\|_{L^2}^2) + \|\phi_r^1\|_{L^2}^2 \right) \tag{76}$$

Note that changing the number of finite element nodes and keeping the number of time steps constant yields similar results. Theoretically, we showed the scaling factors should remain bounded, and these computational results support that. For the computations in Sections 5.2 and 5.3, we note that for larger values of r some of the projection errors, ROM errors, and error formulas become extremely small. In such cases, some of the computed scaling factors are very large, but we believe this is caused by round off errors.

We also include a comparison between the actual error and the error formula for two cases. Table 8 shows the actual error err_1, error formula, and scaling factor C_1. Similarly, Table 9 gives the actual error err_2, the error formula, and the scaling factor C_2. Note that the actual errors and error formulas associated with scaling factors C_4, C_5, and C_6 behave similarly to those associated with C_1 while the actual error and error formula associated with C_3 behaves similarly to those of C_2. The behavior of the values of the actual errors and error formulas as Δt tends to zero is not obvious and would be of interest to study in more detail; we leave this to be considered elsewhere.

Table 8 Error comparison as Δt changes for the ROM error and error formula for C_1

Δt	1/40	1/50	1/100	1/200	1/300
err_1	4.7e–09	1.1e–08	1.0e–07	4.9e–07	9.3e–07
Error formula	8.2e–08	2.2e–07	2.9e–06	1.7e–05	3.8e–05
C_1	5.8e–02	5.1e–02	3.7e–02	2.8e–02	2.5e–02

Table 9 Error comparison as Δt changes for the ROM error and error formula for C_2

Δt	1/40	1/50	1/100	1/200	1/300
err_2	6.7e–07	1.6e–06	1.4e–05	6.5e–05	1.3e–04
Error formula	6.6e–02	1.1e–01	4.8e–01	1.6e00	2.9e00
C_2	1.0e–05	1.4e–05	2.9e–05	4.0e–05	4.3e–05

6 Conclusion

In this work, we introduce a new approach to POD using the difference quotients of the snapshot data. Specifically, we derive the POD modes from a data set that includes only the first snapshot and the regular difference quotients. This data set has approximately half the number of snapshots as the standard POD with DQ approach; also, this data set does not include redundant data when the snapshots are linearly independent. For this new approach to POD with DQs, we prove an approximation result for the weighted sum of the POD projection errors of the regular snapshots, and we also prove that we retain all of the numerical analysis benefits of using DQs that were shown in [29] for the standard POD with DQ approach. Our numerical experiments for a heat equation test problem show that this new approach produces similar reduced order model errors to other known POD approaches.

This work focuses on numerical analysis results concerning pointwise POD projection errors and the optimality of pointwise in time ROM errors for our new approach to POD with DQs. Further investigation is needed to determine how this new approach compares to other standard POD methods in practical computations. The size of the ROM errors is not considered here and more research is needed to compare the size of the ROM error in this case with those of standard POD and standard DQ POD.

Furthermore, we did not theoretically explore here how the new POD DQ approach and the corresponding approximation results, POD projection errors, and ROM errors depend on the time step. Investigating convergence results as the time step tends to zero is of interest and is left to be studied elsewhere.

In this work, we consider only one PDE and one choice of difference quotient. We focus on the heat equation and leave the Navier-Stokes equations and other more complicated PDEs to be considered elsewhere. Additionally, in this work we consider the difference quotients obtained when using backward Euler for time stepping. Other difference quotients are possible and have been used for snapshot collection in [14, 24, 50]. It is possible that results in this paper can be extended to these other difference quotients, but we leave that to be considered elsewhere.

Funding J. Singler was supported by the US National Science Foundation (NSF) under grant number 2111421.

Declarations

Competing interests The authors declare no competing interests.

References

1. Alla, A., Falcone, M., Volkwein, S.: Error analysis for POD approximations of infinite horizon problems via the dynamic programming approach. SIAM J. Control Optim. **55**(5), 3091–3115 (2017). https://doi.org/10.1137/15M1039596
2. Baker, C.G., Gallivan, K.A., Van Dooren, P.: Low-rank incremental methods for computing dominant singular subspaces. Linear Algebra Appl. **436**(8), 2866–2888 (2012). https://doi.org/10.1016/j.laa.2011.07.018
3. Bergmann, M., Cordier, L., Brancher, J.P.: Optimal rotary control of the cylinder wake using proper orthogonal decomposition reduced-order model. Phys. Fluids **17**(9), 097101 (2005). https://doi.org/10.1063/1.2033624
4. Brand, M.: Fast low-rank modifications of the thin singular value decomposition. Linear Algebra Appl. **415**(1), 20–30 (2006). https://doi.org/10.1016/j.laa.2005.07.021
5. Chapelle, D., Gariah, A., Sainte-Marie, J.: Galerkin approximation with proper orthogonal decomposition: new error estimates and illustrative examples. ESAIM Math. Model. Numer. Anal. **46**(4), 731–757 (2012). https://doi.org/10.1051/m2an/2011053
6. Djouadi, S.M.: On the optimality of the proper orthogonal decomposition and balanced truncation. In: Proceedings of the 47th IEEE conference on decision and control, pp. 4221–4226 (2008)
7. Fareed, H., Singler, J.R.: Error analysis of an incremental proper orthogonal decomposition algorithm for PDE simulation data. J. Comput. Appl. Math. **368**, 112525 (2020). https://doi.org/10.1016/j.cam.2019.112525
8. Fareed, H., Singler, J.R., Zhang, Y., Shen, J.: Incremental proper orthogonal decomposition for PDE simulation data. Comput. Math. Appl. Int. J. **75**(6), 1942–1960 (2018). https://doi.org/10.1016/j.camwa.2017.09.012
9. Galán del Sastre, P., Bermejo, R.: Error estimates of proper orthogonal decomposition eigenvectors and Galerkin projection for a general dynamical system arising in fluid models. Numer. Math. **110**(1), 49–81 (2008). https://doi.org/10.1007/s00211-008-0155-9
10. Gohberg, I., Goldberg, S., Kaashoek, M.A.: Classes of linear operators, vol. I, Volume 49 of Operator Theory: Advances and Applications. Birkhäuser Verlag, Basel (1990)
11. Gräßle, C., Hinze, M., Lang, J., Ullmann, S.: POD model order reduction with space-adapted snapshots for incompressible flows. Adv. Comput. Math. **45**(5-6), 2401–2428 (2019). https://doi.org/10.1007/s10444-019-09716-7
12. Gu, H., Xin, J., Zhang, Z.: Error estimates for a POD method for solving viscous g-equations in incompressible cellular flows. SIAM J. Sci. Comput. **43**(1), A636–A662 (2021). https://doi.org/10.1137/19M1241854
13. Gubisch, M., Volkwein, S.: Proper orthogonal decomposition for linear-quadratic optimal control, model reduction and approximation, of Comput. Sci. Eng., vol. 15, pp. 3–63,. SIAM, Philadelphia (2017). https://doi.org/10.1137/1.9781611974829.ch1
14. Herkt, S., Hinze, M., Pinnau, R.: Convergence analysis of Galerkin POD for linear second order evolution equations. Electron. Trans. Numer. Anal. **40**, 321–337 (2013)
15. Higham, J.E., Shahnam, M., Vaidheeswaran, A.: Using a proper orthogonal decomposition to elucidate features in granular flows. Granul. Matter 22(4). https://doi.org/10.1007/s10035-020-01037-7 (2020)
16. Hijazi, S., Stabile, G., Mola, A., Rozza, G.: Data-driven POD-Galerkin reduced order model for turbulent flows. J. Comput. Phys. **416**, 109513 (2020). https://doi.org/10.1016/j.jcp.2020.109513
17. Himpe, C., Leibner, T., Rave, S.: Hierarchical approximate proper orthogonal decomposition. SIAM J. Sci. Comput. **40**(5), A3267–A3292 (2018). https://doi.org/10.1137/16M1085413
18. Hinze, M., Volkwein, S.: Proper orthogonal decomposition surrogate models for nonlinear dynamical systems: error estimates and suboptimal control. Lect. Notes in Comput Sci Eng, pp. 261–306. Springer. https://doi.org/10.1007/3-540-27909-1_10 (2005)
19. Holmes, P., Lumley, J.L., Berkooz, G., Rowley, C.W. Turbulence, coherent structures dynamical systems and symmetry, 2nd edn. Cambridge Monographs on Mechanics. Cambridge University Press, Cambridge (2012)
20. Hömberg, D., Volkwein, S.: Control of laser surface hardening by a reduced-order approach using proper orthogonal decomposition. Math. Comput. Model. **38**(10), 1003–1028 (2003). https://doi.org/10.1016/S0895-7177(03)90102-6

21. Iliescu, T., Wang, Z.: Variational multiscale proper orthogonal decomposition: convection-dominated convection-diffusion-reaction equations. Math. Comp. **82**(283), 1357–1378 (2013). https://doi.org/10.1090/S0025-5718-2013-02683-X
22. Iliescu, T., Wang, Z.: Are the snapshot difference quotients needed in the proper orthogonal decomposition? SIAM J. Sci. Comput. **36**(3), A1221–A1250 (2014a). https://doi.org/10.1137/130925141
23. Iliescu, T., Wang, Z.: Variational multiscale proper orthogonal decomposition: Navier-Stokes equations. Numer. Methods Partial Differ. Equ. **30**(2), 641–663 (2014b). https://doi.org/10.1002/num.21835
24. Jin, B., Zhou, Z.: An analysis of Galerkin proper orthogonal decomposition for subdiffusion. ESAIM Math. Model. Numer. Anal. **51**(1), 89–113 (2017). https://doi.org/10.1051/m2an/2016017
25. Karasözen, B., Uzunca, M.: Energy preserving model order reduction of the nonlinear schrödinger equation. Adv. Comput. Math. **44**(6), 1769–1796 (2018). https://doi.org/10.1007/s10444-018-9593-9
26. Kato, T.: Perturbation theory for linear operators. Classics in Mathematics. Springer, Berlin (1995). Reprint of the 1980 edition
27. Kean, K., Schneier, M.: Error analysis of supremizer pressure recovery for POD based reduced-order models of the time-dependent Navier-STokes equations. SIAM J. Numer. Anal. **58**(4), 2235–2264 (2020). https://doi.org/10.1137/19M128702X
28. Koc, B., Mohebujjaman, M., Mou, C., Iliescu, T.: Commutation error in reduced order modeling of fluid flows. Adv. Comput. Math. **45**(5-6), 2587–2621 (2019). https://doi.org/10.1007/s10444-019-09739-0
29. Koc, B., Rubino, S., Schneier, M., Singler, J.R., Iliescu, T.: On optimal pointwise in time error bounds and difference quotients for the proper orthogonal decomposition. SIAM J. Numer. Anal. **59**(4), 2163–2196 (2021). https://doi.org/10.1137/20M1371798
30. Kostova-Vassilevska, T., Oxberry, G.M.: Model reduction of dynamical systems by proper orthogonal decomposition: error bounds and comparison of methods using snapshots from the solution and the time derivatives. J. Comput. Appl. Math. **330**, 553–573 (2018)
31. Kunisch, K., Volkwein, S.: Galerkin proper orthogonal decomposition methods for parabolic problems. Numer. Math. **90**(1), 117–148 (2001). https://doi.org/10.1007/s002110100282
32. Kunisch, K., Volkwein, S.: Galerkin proper orthogonal decomposition methods for a general equation in fluid dynamics. SIAM J. Numer. Anal. **40**(2), 492–515 (2002). https://doi.org/10.1137/S0036142900382612
33. Kunisch, K., Volkwein, S.: Proper orthogonal decomposition for optimality systems. M2AN Math. Model. Numer. Anal. **42**(1), 1–23 (2008). https://doi.org/10.1051/m2an:2007054
34. Lax, P.D.: Functional analysis. Pure and Applied Mathematics. Wiley-Interscience [Wiley], New York (2002)
35. Leibfritz, F., Volkwein, S.: Numerical feedback controller design for PDE systems using model reduction: techniques and case studies, Real-time PDE-constrained optimization, of Comput. Sci. Eng., vol. 3, pp. 53–72. SIAM, Philadelphia (2007). https://doi.org/10.1137/1.9780898718935.ch3
36. Liang, Y.C., Lee, H.P., Lim, S.P., Lin, W.Z., Lee, K.H., Wu, C.G.: Proper orthogonal decomposition and its applications. I. Theory. J. Sound Vib. **252**(3), 527–544 (2002). https://doi.org/10.1006/jsvi.2001.4041
37. Locke, S., Singler, J.: New proper orthogonal decomposition approximation theory for PDE solution data. SIAM J. Numer. Anal. **58**(6), 3251–3285 (2020). https://doi.org/10.1137/19M1297002
38. Luo, Z., Chen, J., Navon, I.M., Yang, X.: Mixed finite element formulation and error estimates based on proper orthogonal decomposition for the nonstationary Navier-Stokes equations. SIAM J. Numer. Anal. **47**(1), 1–19 (2008/09). https://doi.org/10.1137/070689498
39. Nguyen, V.B., Dou, H.S., Willcox, K., Khoo, B.C.: Model order reduction for reacting flows: laminar Gaussian flame applications. In: 30th international symposium on shock waves vol. 1, pp. 337–343. Springer International Publishing (2017). https://doi.org/10.1007/978-3-319-46213-4_57
40. Quarteroni, A., Manzoni, A., Negri, F.: Reduced basis methods for partial differential equations volume 92 of Unitext. Springer, Cham (2016)
41. Rathinam, M., Petzold, L.R.: A new look at proper orthogonal decomposition. SIAM J. Numer. Anal. **41**(5), 1893–1925 (2003). https://doi.org/10.1137/S0036142901389049
42. Reed, M., Simon, B. Methods of modern mathematical physics I: functional analysis, 2nd edn. Academic Press, Inc., New York (1980)

43. Rowley, C.W.: Model reduction for fluids, using balanced proper orthogonal decomposition. Internat. J. Bifur. Chaos Appl. Sci. Engrg. **15**(3), 997–1013 (2005). https://doi.org/10.1142/S0218127405012429
44. Rubino, S.: A streamline derivative POD-ROM for advection-diffusion-reaction equations. ESAIM: Proc. Surv. **64**, 121–136 (2018). https://doi.org/10.1051/proc/201864121
45. Sachs, E.W., Schu, M.: A priori error estimates for reduced order models in finance. ESAIM Math. Model. Numer. Anal. **47**(2), 449–469 (2013). https://doi.org/10.1051/m2an/2012039
46. Singler, J.R.: Convergent snapshot algorithms for infinite-dimensional Lyapunov equations. IMA J. Numer. Anal. **31**(4), 1468–1496 (2011). https://doi.org/10.1093/imanum/drq028
47. Singler, J.R.: New POD error expressions, error bounds, and asymptotic results for reduced order models of parabolic PDEs. SIAM J. Numer. Anal. **52**(2), 852–876 (2014). https://doi.org/10.1137/120886947
48. Volkwein, S.: Interpretation of proper orthogonal decomposition as singular value decomposition and HJB-based feedback design. In: Proceedings of the 16th international symposium on mathematical theory of networks and systems (MTNS) (2004)
49. Willcox, K., Peraire, J.: Balanced model reduction via the proper orthogonal decomposition. AIAA J. **40**(11), 2323–2330 (2002). https://doi.org/10.2514/2.1570
50. Zhu, S., Dedè, L., Quarteroni, A.: Isogeometric analysis and proper orthogonal decomposition for the acoustic wave equation. ESAIM Math. Model. Numer. Anal. **51**(4), 1197–1221 (2017). https://doi.org/10.1051/m2an/2016056